AFOSR Interim Scientific Report

ON THE PROPAGATION OF SPHERICAL DETONATION WAVES

by

J.H. Lee

G.G. Bach

MERL Report 72-9

Research sponsored by Air Force Office of Scientific Research

United States Air Force

Col. B.W. Haffner AFOSR Technical Monitor

AFOSR Grant 69-1752B

Department of Mechanical Engineering

McGill University

Montreal, Canada

July 1972

UNCLASSIFIED

Security Classification

DOCUMENT CONTROL DATA - R & D

(Security classification of title, body of abstract and indexing annotation must be entered when the overall report is classified)

1. ORIGINATING ACTIVITY (Corporate author)	2a. REPORT SECURITY CLASSIFICATION
MCGILL UNIVERSITY DEPARTMENT OF MECHANICAL ENGINEERING MONTREAL 110, P.Q., CANADA	UNCLASSIFIED 2b. GROUP

3. REPORT TITLE

ON THE PROPAGATION OF SPHERICAL DETONATION WAVES

4. DESCRIPTIVE NOTES (Type of report and inclusive dates)

Scientific Interim

5. AUTHOR(S) (First name, middle initial, last name)

GLEN G BACH JOHN H LEE

6. REPORT DATE	7a. TOTAL NO. OF PAGES	7b. NO. OF REFS
July 1972	37	26

8a. CONTRACT OR GRANT NO.	9a. ORIGINATOR'S REPORT NUMBER(S)
AFOSR-69-1752	MERL Report 72-9
b. PROJECT NO. 9711-01	
c. 61102F	9b. OTHER REPORT NO(S) (Any other numbers that may be assigned this report) AFOSR TR 73-1978
d. 681308	

10. DISTRIBUTION STATEMENT

Approved for public release; distribution unlimited.

11. SUPPLEMENTARY NOTES	12. SPONSORING MILITARY ACTIVITY
TECH, OTHER	AF Office of Scientific Research (NAE) 1400 Wilson Boulevard Arlington, Virginia 22209

13. ABSTRACT

A novel theory for the propagation of a spherical detonation wave is presented. The model is that of a point spherical blast in a detonating medium. The reaction rates are assumed to be finite but the coupling between the shock motion and the chemical reactions is modelled by a global function which leads to an effective chemical energy release at the detonation front which depends on the local shock strength and the shock radius. The important result obtained is the demonstration of the existence of finite steady-state velocities which are below the theoretical planar Chapman-Jouguet value. The magnitude of these final steady-state velocities depends on the value of the ignition energy used to initiate the detonation wave itself. A quantitative comparison with the recent velocity measurements made by Brossard in stoichiometric and equi-molar C_2H_2-O_2 mixtures at $.1 \leq P_o \leq .28$ bar showed good agreement, lending support to the present proposed theory. Using the experimental data of White for the induction time, the present theory can be used to predict the critical energy for direct initiation as well as the transverse wave spacing, and both are found to be in good agreement with the experimental data.

1

DD FORM 1 NOV 65 1473

UNCLASSIFIED

Security Classification

14 KEY WORDS	LINK A		LINK B		LINK C	
	ROLE	WT	ROLE	WT	ROLE	WT
THEORY						
PROPAGATION						
SPHERICAL GASEOUS DETONATIONS						

AFOSR Scientific Report

ON THE PROPAGATION OF SPHERICAL DETONATION WAVES

by

G.G. Bach

J.H. Lee

MERL Report 72-9

Progress report for research sponsored in part by the United States Air Force Office of Scientific Research, Col. R.W. Haffner, Technical Monitor under AFOSR Grant 69-1752B and by the National Research Council of Canada under Grants A-3347, A-118 and A-6819.

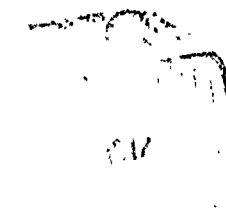

Department of Mechanical Engineering
McGill University
Montreal, Canada

July 1972

Abstract

A novel theory for the propagation of a spherical detonation wave is presented. The model is that of a point spherical blast in a detonating medium. The reaction rates are assumed to be finite but the coupling between the shock motion and the chemical reactions is modelled by a global function which leads to an effective chemical energy release at the detonation front which depends on the local shock strength and the shock radius. The important result obtained is the demonstration of the existence of finite steady-state velocities which are below the theoretical planar Chapman-Jouguet value. The magnitude of these final steady-state velocities depends on the value of the ignition energy used to initiate the detonation wave itself. A quantitative comparison with the recent velocity measurements made by Brossard in stoichiometric and equi-molar C_2H_2-O_2 mixtures at $.1 \leq p_o \leq .28$ bar showed good agreement, lending support to the present proposed theory. Using the experimental data of White for the induction time, the present theory can be used to predict the critical energy for direct initiation as well as the transverse wave spacing, and both are found to be in good agreement with the experimental data.

1. Introduction

From the theoretical point of view, the existence of Chapman-Jouguet (C-J) spherical detonation waves depends on the existence of a physically acceptable solution to the unsteady gasdynamic equations that satisfies the C-J boundary conditions at the detonation front. The early studies by Jouguet [1], Taylor [2] and Zeldovich [3] (J-T-Z) were based on the idealized model of a discontinuous C-J front originating at the center $r = 0$ at time $t = 0$ and subsequently expanding outwards at a constant velocity. The similarity solution they obtained possesses a singularity in the form of an infinite expansion gradient immediately behind the detonation front. The presence of this singularity throws some doubts as to the validity of the J-T-Z solution on a physical basis, hence the existence of spherical C-J detonations is not established by the J-T-Z model.

Recognizing the experimental fact that the direct initiation of a spherical detonation wave invariably demands the explosive release of a finite quantity of energy, the reacting blast wave model (R-B-W) was subsequently proposed and analysed by Lee [4]. The detonation front is still treated as a gasdynamic discontinuity but with the inclusion of a finite initiation energy E_0, no steady wave solution is possible. The detonation front is initially highly overdriven and propagates essentially as a strong point blast wave (i.e., $R_s \sim t^{2/5}$). As the wave expands, the effect of chemical energy release at the front progressively influences the wave motion until a C-J wave is approached asymptotically as $R_s \to \infty$. A later study of the R-B-W model by Korobeinikov [5] using a perturbation method demonstrated a similar

behaviour. Hence according to the R-B-W model, no steady state spherical C-J detonation waves are possible.

In a recent study by Levin and Chernyi [6] on the asymptotic motion of a decaying overdriven spherical detonation, it is found that unlike the decay of a non-reacting blast, the final steady state C-J condition can be achieved at a finite radius. A more careful subsequent analysis by the Authors [7] indicates that although Levin and Chernyi's solution is possible, there are no convincing arguments on a physical basis in the assumption of the particular asymptotic behaviour of the flow structure which is necessary to arrive at their result. Also, Levin and Chernyi's analysis assumes the J-T-Z similarity solution when the C-J condition is reached. From the solution for the R-B-W model there seems to be no indication that it would approach the J-T-Z similarity solution as the decaying overdriven wave becomes a C-J wave. An attempt to verify Levin and Chernyi's asymptotic solution by carrying out a numerical characteristic analysis of the R-B-W model to the asymptotic regime is inconclusive as instability of the type obtained by Fickett and Wood [8] and Strehlow and Hartung [9] occurs when the C-J conditions are approached. Hence no definite conclusions can be drawn at this stage. However, even if the Levin and Chernyi solution does provide the asymptotic motion of the detonation wave in the R-B-W model, the physically questionable J-T-Z similarity solution is still retained.

In the J-T-Z and R-B-W models, the chemical reaction rates have been assumed to be sufficiently fast so that the detonation front can be considered as a gasdynamic discontinuity. In the recent studies

by the Authors [10] and Lundstrom and Oppenheim [11], it is demonstrated that the rapid gasdynamic expansion immediately behind a spherical blast wave can result in a significant increase in the reaction zone thickness. Hence it is quite evident that the discontinuity assumption for the detonation front would have to be abandoned in a realistic theoretical model. Unfortunately, a finite kinetic rate model where strong coupling exists between the hydrodynamics and the chemical reactions is extremely complex mathematically. The numerical studies thus far by Rajan [12] and Taki and Fujiwara [13] provide only a partial description of the problem in the overdriven regime of the shock motion. Instability problems near the C-J regime of the shock motion would be the major difficulty in any numerical solution of the exact model. It is also doubtful that shock tube kinetic data can be used in these exact models for spherical detonations since the molecular energy transfer processes occur under highly non-equilibrium conditions [14]. In an attempt to reproduce qualitatively the experimental observations for the propagation of a spherical detonation wave, a simple phenomenological model was proposed by the Authors in a recent paper [15]. There the coupling between the chemical energy release in the flow structure and the motion of the expanding detonation front is assumed to depend on the local induction zone thickness. The dependence of the induction zone thickness on the local shock strength and the flow gradient is modelled globally by an appropriate mathematical functions. The results of that preliminary study are extremely encouraging in that almost all the essential features of the propagation of a spherical detonation wave observed experimentally are reproduced on a qualitative basis. The present paper describes our

subsequent work on this phenomenological theory. Adopting essentially the same approach, the previous model has been completely reformulated and analysed in the present paper. The results of the present model can now be compared with experiments on a quantitative basis.

2. Formulation

As in the R-B-W model, we consider the propagation of a point spherical blast wave in a detonating gas. The blast is generated by the instantaneous deposition of a finite quantity of energy E_o at the origin at time $t = o$. However, unlike the J-T-Z or the R-B-W model the chemical kinetic rates are now considered to be finite so that at any instant of time t when the shock is at a radius $R_s(t)$, the reaction front is at $R_s(t) - d(t)$ lagging behind the shock by a distance $d(t)$. The present model does not assume a weak coupling between the hydrodynamic and the chemical reactions. Therefore the description of the shock motion and the reaction kinetics in the flow behind the shock cannot be determined independently as in the previous studies of the finite kinetic rate blast model [10, 11]. However, instead of seeking a complete solution to the problem, which would require the simultaneous solution of the non-linear hydrodynamic equations and the appropriate kinetic rate equations, we are interested in the motion of the detonation wave only. In other words, we are not concerned with the determination of the detailed hydrodynamic flow structure and the distributions of the various chemical species in the wake of the spherical detonation front, but only in the shock trajectory $R_s(t)$ and the variation of the strength of the detonation wave with radius. Within

the context of this modest aim, certain simplifying assumptions can be made, resulting in a considerable reduction in mathematical difficulties.

First of all, we note from the well-known blast wave theory that the shock trajectory $R_s(t)$ is rather insensitive to the manner in which the flow properties (i.e., pressure p, density ρ and particle velocity u) are distributed behind the shock provided that the global conservation laws are satisfied. By global conservation laws, we mean the integral relationships for the conservation of mass, i.e.,

$$\int_0^{R_s(t)} 4\pi r^2 \rho \, dr = \int_0^{R_s(t)} 4\pi r^2 \rho_0 \, dr = \frac{4\pi}{3} \rho_0 R_s^3(t) \tag{2.1}$$

and the conservation of energy

$$E_0 = \int_0^{R_s(t)} 4\pi r^2 \left(e + \frac{u^2}{2}\right) \rho \, dr - \int_0^{R_s(t)} 4\pi r^2 \rho_0 e_0 \, dr - \int_0^{R_s(t)-d(t)} 4\pi r^2 \rho Q \, dr \tag{2.2}$$

where e and Q denote the internal thermal energy and the chemical energy per unit mass respectively, and the subscript " 0 " represents the initial undisturbed condition. Since the flow is spherically symmetric, the total momentum is always zero and is conserved automatically. For blast waves, the most important relationship is the energy integral. The insensitivity of the shock trajectory $R_s(t)$ to the flow structure is noticed from the fact that though the flow distributions differ significantly in the various non-similar solutions for the blast wave

problem , the results for the shock trajectory are almost identical [16, 17, 18]. It should be noted that in the non-similar solution of Oshima [17], the mass integral is not even satisfied. However, by requiring that the total energy is conserved, Oshima's solution for the shock trajectory is quite accurate when compared to the more rigorous solution of Sakurai' [16] where both the mass and energy are conserved.

Based on the insensitivity of the shock trajectory on the flow distributions, we therefore ignore the influence of the chemical reactions on the hydrodynamic flow structure and assume the density, particle velocity and pressure profiles behind the spherical wave as

$$\rho(r,t) = \rho_1(R_s,t)\left(\frac{r}{R_s}\right)^{g(t)} \tag{2.3}$$

$$u(r,t) = \dot{R}_s\left(\frac{r}{R_s}\right) \tag{2.4}$$

$$p(r,t) = p_0 + \dot{R}_s^2\frac{\rho_1(R_s,t)}{g(t)+2}\left(1-\left(\frac{r}{R_s}\right)^{g(t)+2}\right)\cdot$$
$$\cdot\left[\frac{R_s\ddot{R}_s m_s}{\dot{R}_s^2}\frac{d}{dm_s}\left(\frac{u_1(R_s,t)}{\dot{R}_s}\right) - \frac{u_1(R_s,t)}{\dot{R}_s}\left(1-\frac{u_1(R_s,t)}{\dot{R}_s}-\frac{R_s\ddot{R}_s}{\dot{R}_s^2}\right)\right] \tag{2.5}$$

where $\dot{R}_s$, $\ddot{R}_s$ denote the first and second derivative of R_s with respect to time. The above forms for the flow distributions are essentially those for a non-reacting blast wave [18] and they satisfy

the conservation integrals. The exponent $g(t)$ for the density profile given by Eq. 2.3 can be evaluated from the mass integral (i.e., Eq. 2.1) as

$$g(t) = 3\left(\frac{\rho_1(R_s,t)}{\rho_0} - 1\right) \tag{2.6}$$

where the subscript " 1 " denotes the condition at the shock front. By assuming the flow structure to be as specified by Eqs. 2.3 to 2.5, we no longer have to concern ourselves with the hydrodynamic conservation equations.

With the induction zone thickness $d(t)$ finite, the total chemical energy released in the flow at any instant will be given by the integral

$$\int_0^{R_s(t)-d(t)} 4\pi r^2 \rho Q\, dr$$

The second approximation used in the present model is to consider the shock as reactive, but with chemical energy $Q_e(t)$ per unit mass released instantaneously at the front $r = R_s(t)$ instead of the total chemical energy per unit mass of the mixture Q in the J-T-Z and R-B-W models. This effective chemical energy $Q_e(t)$ depends on the local induction zone thickness and the dependence can be obtained by considering the conservation of chemical energy at any instant of time, i.e.,

$$\int_0^{R_s(t)-d(t)} 4\pi r^2 \rho Q\, dr = \int_0^{R_s(t)} 4\pi r^2 \rho_0 Q_e(t)\, dr$$

Using Eqs. 2.3 and 2.6, the effective chemical energy $Q_e(t)$ can

be obtained as

$$Q_e(t) = Q\left(1 - \frac{d(t)}{R_s(t)}\right)^{\gamma(t)+3} \tag{2.7}$$

If the induction zone thickness $d(t) \to 0$, then $Q_e \to Q$ and the present model reduces to the R-B-W model for a discontinuity detonation front. The coupling between the shock motion and chemical reactions is essentially described by the relationship Eq. 2.7. The degree of coupling depends on the induction zone thickness $d(t)$.

With the effective chemical energy $Q_e(t)$ released at the shock front instantaneously, the boundary conditions can be written as

$$\frac{p_1(R_s,t)}{p_0} = \frac{\gamma+1}{\gamma-S+\eta} \tag{2.8}$$

$$\frac{u_1(R_s,t)}{\dot{R}_s(t)} = \frac{1+S-\eta}{\gamma+1} \tag{2.9}$$

$$\frac{p_1(R_s,t)}{p_0 \dot{R}_s^2(t)} = \frac{\gamma+\gamma S+\eta}{\gamma(\gamma+1)} \tag{2.10}$$

where

$$S = \left\{(1-\eta)^2 - k\eta\right\}^{1/2} \tag{2.11}$$

$$K = \frac{2(\gamma^2-1)Q_e(t)}{C_0^2} \tag{2.12}$$

and

$$\eta = \frac{1}{M_S^2} = \frac{C_0^2}{\dot{R}_S^2} = \frac{\gamma p_0}{\rho_0}\cdot\frac{1}{\dot{R}_S^2} \tag{2.13}$$

Note that there are two roots for S from Eq. 2.11 with the positive root representing the overdriven detonation solution and the negative root for the weak detonation solution. The unique solution for $S = 0$ corresponds to the C-J solution. The positive root for S is used in the present analysis since we are concerned with the decay of an initially overdriven wave to its final steady state velocity when $S = 0$. Since $Q_e(t)$ is a function of the shock radius, the final steady state velocity depends on the solution $R_S(t)$ and the magnitude of $Q_e(t)$ is determined when $S = 0$.

The third approximation in the formulation of the present model is the specification of the functional form for the induction zone thickness $d(t)$. From the results of the previous study of the finite kinetic rate blast model [10, 15] and experimental observations, the following form is chosen

$$d(t) = \Delta(1 - e^{-\chi z^3}) \tag{2.14}$$

where

$$z = \frac{Q}{3C_0^2} \tag{2.15}$$

$$z = R_s/R_0 \tag{2.16}$$

and R_0 is the characteristic explosion length commonly used in blast wave scaling defined as

$$R_0 = \left(\frac{E_0}{4\pi C_0^2 \rho_0}\right)^{1/3} \tag{2.17}$$

Writing the exponent χz^3 in Eq. 2.14 in terms of the fundamental parameters, we see that

$$\chi z^3 = \frac{\frac{4}{3}\pi \rho_0 Q R_s^3}{E_0}$$

which is simply the ratio of the total chemical energy to the initiation at any instant of time. When $\chi z^3 << 1$, the shock motion is dominated by the initiation energy E_0 and the front is essentially a strong shock and $d(t) \to 0$. When $\chi z^3 >> 1$ the chemical energy dominates the shock motion and $d(t) \to \Delta$ which is some constant depending on the particular magnitude of final steady state shock strength of the solution. Both these limiting behaviours as well as the exponential nature of $d(t)$ given by Eq. 2.14 correspond to experimental observations.

As a final step in the formulation of the model, a lower limiting shock strength where chemical reactions are completely decoupled from the shock motion has to be specified. This is based on the existence of a temperature limit below which auto-ignition of the gas behind the shock is no longer possible. This limit is ill-

defined experimentally, but for most practical gaseous explosives of interest, the limiting temperature is of the order of $1000^{\circ}K$. In the present study we shall take a critical shock strength $M_c = 3$ for the lower limit. In other words, if the shock decays below in any particular solution, we will completely decouple any chemical reactions from the shock motion. Hence we set the limiting conditions for Eq. 2.7 as

$$Q_e = Q F(\eta, z)$$

$$F(\eta, z) = \left(1 - \frac{d(t)}{R_s(t)}\right)^{\gamma(\gamma+1)+3}, \quad \eta \leq \eta_c \qquad (2.18)$$

$$= 0, \quad \eta \geq \eta_c$$

It should be noted that the "cut-off" specified in Eq. 2.18 is an abrupt step-function type of behaviour while in reality it is a smooth function. However, due to the sharp exponential increase of $d(t)$ near the auto-ignition limit, the assumed step function behaviour is quite justified. The essential steps in the formulation of the present model have now been specified.

3. Analysis

For convenience in the analysis and numerical computations, we shall recast the basic equations in the previous section in the familiar blast wave parameters [18]. Replacing the independent

variables (r , t) by (ξ, η) where

$$\xi = r/R_s(t)$$

$$\eta = \frac{1}{m_s^2} = \frac{c_0^2}{\dot{R}_s^2} = \frac{\gamma p_0}{\rho_0} \cdot \frac{1}{\dot{R}_s^2} \tag{3.1}$$

and the dependent variables (p , ρ , u) by (f , ψ , ϕ) where

$$f(\xi, \eta) = \frac{p(r,t)}{\rho_0 \dot{R}_s^2}$$

$$\psi(\xi, \eta) = \frac{\rho(r,t)}{\rho_0} \tag{3.2}$$

$$\phi(\xi, \eta) = \frac{u(r,t)}{\dot{R}_s}$$

The density, particle velocity and the pressure profiles behind the spherical wave as given previously by Eqs. 2.3 to 2.5 become

$$\psi = \psi_1(1,\eta)\xi^\delta \tag{3.3}$$

$$\phi = \phi_1(1,\eta)\xi \tag{3.4}$$

$$f = f_1(1,\eta) - \frac{\psi_1(1-\xi^{\delta+2})}{\delta+2}\left(2\theta\eta\frac{d\phi_1}{d\eta} + \phi_1(1-\phi_1-\theta)\right) \tag{3.5}$$

where

$$\theta = R_s \ddot{R}_s / \dot{R}_s^2 \tag{3.6}$$

The parameter θ denotes whether the shock is decelerating $\theta < 0$ or accelerating $\theta > 0$. The exponent $g(t)$ of the density profile in Eq. 3.3 can be written in terms of the blast wave parameters as

$$g(\eta) = 3(\psi_1(1,\eta) - 1) \tag{3.7}$$

The subscript 1 in Eqs. 3.3 to 3.5 denotes the conditions immediately behind the shock front and ψ_1, ϕ_1, f_1 are given previously by Eqs. 2.8 to 2.10.

Substituting the profiles for ϕ, f and ψ into the energy integral, we obtain the following equation

$$1 = \frac{z^3}{\eta}\left[\frac{f_1}{3(\gamma-1)} - \frac{\psi_1\phi_1(1-\phi_1)}{3(\gamma-1)(g+5)} + \frac{\psi_1\phi_1^2}{2(g+5)}\right.$$
$$\left. - \frac{\psi_1\left(2\eta\frac{d\phi_1}{d\eta} - \phi_1\right)\theta}{3(\gamma-1)(g+5)}\right]$$
$$- z^3\left[\frac{1}{3\gamma(\gamma-1)} + \varepsilon\left(1 - \frac{d(t)}{R_s(t)}\right)^{g+3}\right] \tag{3.8}$$

where ε, z and R_0 are defined previously by Eqs. 2.15 to 2.17 respectively. From the definition of θ given by Eq. 3.6, we obtain the relationship

$$\frac{d\eta}{dz} = -\frac{2\theta}{z}\eta \tag{3.9}$$

so that the term $d\phi_1/d\eta$ in Eq. 3.8 may be written as

$$\frac{d\phi_1}{d\eta} = \frac{\partial\phi_1}{\partial\eta} + \frac{dz}{d\eta}\frac{\partial\phi_1}{\partial z} = \frac{\partial\phi_1}{\partial\eta} - \frac{z}{2\theta\eta}\frac{\partial\phi_1}{\partial z} \tag{3.10}$$

Evaluating $\partial\phi_1/\partial\eta$ and $\partial\phi_1/\partial z$ from the boundary condition at the front for ϕ_1 (i.e., Eq. 2.9), we obtain

$$\frac{d\phi_1}{d\eta} = -\frac{1}{2S(\gamma+1)}\left(2(1-\eta) + k + \eta k_\eta + 2S - \frac{z}{2\theta}k_z\right) \tag{3.11}$$

where

$$k_\eta = \frac{\partial k}{\partial\eta}$$

$$= \frac{(\gamma+3)\psi_1 k}{2(\gamma+1)} \cdot \frac{(2(1-\eta)+k+2S)\ln(1-\frac{\delta}{2})}{S + \eta(\gamma+3)\frac{k\psi_1}{2(\gamma+1)}\ln(1-\delta/2)} \tag{3.12}$$

and

$$k_z = \frac{\partial k}{\partial z}$$

$$= \frac{(\gamma+3)\epsilon S k}{z^2(1-\delta/2)} \cdot \frac{(1-[1+3z^2z^3]e^{-z^3})}{S + \eta(\gamma+3)\frac{k}{2(\gamma+1)}\psi_1\ln(1-\delta/2)} \tag{3.13}$$

S and k are defined previously by Eqs. 2.11 and 2.12 respectively while δ and ϵ are defined as

$$\epsilon = \Delta/R_0$$

$$\delta = d(t)/R_0 \tag{3.14}$$

Using Eq. 3.10, we can solve for θ from Eq. 3.8 as

$$\theta = \frac{3(\gamma^2-1)(\xi+3)S}{\psi_1(\gamma+1)\phi_1(1+\eta)+\eta^2 k_\eta}\left\{\frac{\eta}{z^3}\left(1+\alpha\left(1-\frac{\delta}{z}\right)^{\xi+3}\right)\right.$$

$$-\frac{\phi_1}{3(\gamma-1)} + \frac{\psi_1\phi_1(1-\phi_1)}{3(\gamma-1)(\xi+3)} - \frac{\psi_1\phi_1^2}{2(\xi+3)} \tag{3.15}$$

$$\left.+\frac{\psi_1 z\eta k_z}{6(\gamma^2-1)(\xi+3)S}\right\}$$

Substituting the above equation into Eq. 3.8, we obtain a differential equation for the change of the shock strength η with the radius z, i.e.,

$$\frac{d\eta}{dz} = G(\eta, z) \tag{3.16}$$

which may be integrated numerically using, for example, the standard Runge-Kutta method.

To start the numerical intergration we must obtain the value of η at some small initial value of z. From Eq. 3.8, we note that as $z \to 0$, $\eta \to z^3$ since the left hand side of the equation is finite. Hence the form of the expansion $\eta(z)$ for small values

of z should be of the form

$$\eta = Az^3 + \cdots \tag{3.17}$$

and from Eq. 3.9, $\theta(z)$ for small values of z is

$$\theta = -3/2 + \cdots \tag{3.18}$$

Substituting the perturbation expressions into Eq. 3.18, the coefficient A can be evaluated as

$$A = \frac{11\gamma - 5}{3(\gamma+1)(5\gamma+1)} \tag{3.19}$$

For some chosen initial value of z, Eqs. 3.17 and 3.18 provide the starting conditions for the numerical integration of Eq. 3.17.

To obtain an expression for the shock trajectory, we note that $\dot{R}_s = dR_s/dt$ and in terms of η and z we can write

$$\frac{c_o t}{R_o} = \int_0^z \eta^{\frac{1}{2}} dz \tag{3.20}$$

For small values of z, we use the perturbation expression for $\eta(z)$ (i.e., Eq. 3.17) and Eq. 3.20 yields

$$\frac{c_o t}{R_o} = \frac{2}{5} A^{\frac{1}{2}} z^{5/2} + \cdots$$

and since $z = R_s/R_o$ we note from the above that $R_s \sim t^{2/5}$. Hence the shock behaves like a strong point blast wave.

For very large initiation energy, $E_0 \to \infty$ or $R_0 \to \infty$ and hence from Eqs. 2.14 and 2.7, $d(t) \to 0$ so that $Q_e \to Q$. In other words, the full chemical energy per unit mass is released instantaneously at the front and the present solution recovers the reacting blast wave model [4, 5, 7]. Alternatively, we can assume the front to be discontinuous by simply taking $\Delta = 0$ and again the reacting blast wave model is recovered. However, in this case, the initiation energy E_0 can be arbitrary and in the limit $E_0 \to 0$, we recover the J-T-Z model.

Taking $Q = 0$, the boundary conditions (i.e., Eqs. 2.8 to 2.10) reduce to the ordinary Rankine-Hugoniot equations for a normal shock in a perfect gas. The present solution then becomes the solution for a non-reacting blast wave [18]. With the non-reacting hydrodynamic flow structure determined, the chemistry of the reactions between the shock can be computed. This in essence is the finite kinetic rate model studied by the Authors [10] and Lundstrom and Oppenheim [11]. Therefore we see that the present model is consistent with and unifies all the previous theoretical models.

4. Results and Discussions

For an explosive mixture at given initial conditions we shall specify the following parameters: the specific heat ratio γ, the initial pressure p_0 and sound speed c_0, the planar C-J Mach No. M_{CJ} (hence the chemical energy per unit mass Q), and the critical shock Mach No. M_c corresponding to the auto-ignition limit of the mixture. For the system $C_2H_2 - O_2$ studied in this paper, we choose $M_c = 3$ which corresponds to an auto-ignition temperature limit $T_c \simeq 1000^\circ K$.

For any chosen value of the initiation energy parameter $\epsilon = \Delta/R_0$, we can obtain the solutions for the shock trajectory $z(t)$ and the variation of shock strength with radius $\eta(z)$ by integrating Eqs. 3.16 and 3.20. To start the numerical integration, the perturbation expressions given by Eqs. 3.17 and 3.18 are used to evaluate the starting values for η and θ for some small chosen value of $z = z_0$. In the present work z_0 was chosen to be 0.05 and the integration was found to proceed smoothly for increasing values of z without oscillations.

It is important to consider first the general properties of the solutions for $\theta(z)$, $\eta(z)$ and $S(z)$ for various values of the initiation energy parameter ϵ. A typical example for the case of stoichiometric $C_2H_2 - O_2$ undiluted mixture at an initial pressure $p_0 = 100$ torr and temperature $T_0 = 300^\circ K$ is shown in Fig. 1. The solutions for $\theta(z)$ for various values of ϵ all start out at the limiting strong shock value of $\theta(0) = -3/2$ and increase towards zero as the shock expands and the influence of the chemical energy release becomes progressively important with larger shock radius z. The

solutions of $S(z)$ all start out at its initial value $S(0) = 1$, which corresponds to the strong shock limit $\eta = 0$ (i.e., $M_s = \infty$) and decrease monotomically to zero as the shock expands and decelerates. From Eq. 3.15, we see that when $S = 0$, the parameter $\theta = 0$, which implies that the shock acceleration $d\dot{R}_s/dt = \ddot{R}_s = 0$. Hence as $S \to 0$, the shock ceases to decelerate and will propagate thereafter at a final steady state velocity M_s^*. Since M_s^* corresponds to $S = 0$, we see from the boundary conditions (i.e., Eqs. 2.8 to 2.10) that this solution is one where the Rayleigh line is tangent to the equilibrium Hugoniot curve for the particular value of Q_e obtained. Hence this final steady state velocity M_s^* can be interpreted as the local C-J velocity. As M_s^* is a function of ϵ, a different final steady state velocity is obtained for different values of the initiation energy parameter ϵ. This implies that for spherical detonations, the final steady state C-J velocity depends on the magnitude of the initiation energy E_o. The present conclusion is then contradictory to the classical theory where, for a given explosive, the steady state C-J velocity depends only on the properties of the explosive itself.

From Fig. 1, it is seen that for small values of ϵ (i.e., large initiation energy) the solutions for $\theta(z)$ and $S(z)$ indicate that $\theta(z) \to 0$ simultaneously as $S(z) \to 0$. However, for larger values of ϵ, we note that $\theta(z) \to 0$ when $S(z)$ is still finite and $\theta(z)$ hence becomes positive and continues to increase as $S(z)$ monotomically decreases to zero. When $S(z) = 0$, the value of $\theta(z)$ becomes multi-value since from Eq. 3.15, θ must vanish when $S = 0$. Physically this implies that the shock over-dece-

lerates at first to a minimum velocity and as $S(\tau)$ is still finite, the shock accelerates again until $S(\tau) = 0$ when the acceleration must suddenly cease (i.e., $\theta = 0$) for the shock to propagate subsequently at a steady state velocity M_s^*. The discontinuous jump in the shock acceleration is illustrated in the large abrupt change in the solution for $\theta(\tau)$ for the case of $\epsilon = 0.13$ shown in Fig. 1. This sudden transition demonstrates a type of instability which occurs when the hydrodynamic flow structure is not coupled smoothly to the chemical reactions. It should be noted that in the numerical studies of the deceleration of an initially planar overdriven detonation wave [8, 9] the onset of instability is also observed as the shock approaches its final steady state C-J condition. This type of instability is inherent in all detonation problems and within the context of the present model, more detailed information on this instability mechanism cannot be obtained. However, for small values of the initiation energy parameter ϵ, the amplitudes of the jumps in $\theta(\tau)$ are sufficiently small and are within the round off errors of the finite step sizes of the numerical integration scheme. Hence we shall assume that for small values of ϵ (i.e., $0 \leq \epsilon \leq .05$ for the particular case shown in Fig. 1) the deceleration of the spherical detonation wave to its final steady state velocity M_s^* is smooth.

The stable behaviour of the solutions for small values of ϵ can best be illustrated by the solutions for $\eta(\tau)$. We note that for the range of $0 \leq \epsilon \leq .05$, the shock strength $\eta(\tau)$ decays smoothly from its initial value $\eta(0) = 0$ to some final steady state value

$\eta(z) = \eta^*$. Outside this range $0 \leq \epsilon \lesssim .05$, the shock decays to a minimum and accelerates again. The transition to its final steady state value η^* when $S = 0$ is discontinuous. This is illustrated clearly for the case $\epsilon = 0.13$. Since for each shock radius z the local value of Q_e can be evaluated from Eqs. 2.7 and 2.14, we can determine the local C-J velocity by taking $S = 0$ and solving for η from Eq. 2.11. The variations of this local C-J value of $\eta'(z)$ with radius for the various values of ϵ are also shown in Fig. 1. We note that the corresponding $\eta(z)$ is always less than the local C-J value of $\eta'(z)$ during the decay (the shock speed is always greater than its local C-J velocity). Hence the detonation wave is overdriven at all times until $S = 0$ when $\eta(z) = \eta'(z) = \eta^*$ and the final steady state velocity is obtained.

In Fig. 2, the variation of the detonation Mach No. $M_S(z)$ with radius $z = R_S/R_0$ is shown. For small shock radii (i.e., $z \ll 1$) where the initiation energy dominates the shock motion, all the curves coalesce and the decay is essentially that of a strong blast (i.e., $M_S \sim 1/z^{3/2}$). For example, all the solutions for $M_S(z)$ are indiscernible from each other for $z \sim 0.2$, which corresponds to the energy ratio

$$\chi z^3 = \frac{4}{3}\pi \frac{\rho_0 Q R_S^3}{E_0} \simeq .08$$

In other words, the total chemical energy enclosed by the wave is about 8% of the initiation energy E_0 only. Significant departures from the blast wave solution should occur when the energy ratio $\chi z^3 \sim 1$ which, for the particular case shown, is at a shock radius $z \simeq .46$

where the differences between the various solutions are quite pronounced. The final steady state conditions (i.e., $M_s \sim M_s^*$) correspond to a shock radius $Z \simeq 0.6$. This yields an energy ratio $\alpha Z^3 \simeq 2$. In other words, when the chemical energy finally dominates the shock motion,

$$\frac{4}{3}\pi \rho_0 Q R_s^3 \simeq 2E_0$$

Although the so-called smooth stable regime $0 \leq \epsilon \leq 0.5$ for the decay to the final steady state velocity is arbitrarily set based on the vanishingly small abrupt change of slope as $M_s(Z) \to M_s^*$, it is interesting to note that this stable limit is in accord with the stability criterion of Shchelkin [19]. Using the final steady state velocity $M_s^* = 5.7$ for the limiting value of $\epsilon = 0.5$, the induction time computed using White's [20] data for this mixture (i.e., $\ln [C_2H_2]^{1/3}[O_2]^{1/3}\tau = -10.81 + 17300/(4.58T)$) is $\tau^* = .056 \times 10^{-6}$ sec., which is about twice the value $\tau_{CJ} = .029 \times 10^{-6}$ sec. for the planar C-J velocity of $M_{CJ} = 7.015$. According to Shchelkin, if a random disturbance results in an increase in the induction time by an order of magnitude equal to or greater than the initial delay time itself, then the detonation front loses its stability. For spherical detonations, the increase in the induction time is due to the lateral expansion associated with the three-dimensional geometry.

For $\epsilon \geq .05$ the detonation wave decays to a minimum and then accelerates again. The transition to its final steady state velocity M_s^* when $S = 0$ is discontinuous. This corresponds to the experimental observations of the propagation of a spherical detonation

wave in the critical initiation energy regime [10]. The detonation decays continuously to a velocity corresponding to the auto-ignition limit of $M_C \simeq 3$. The shock-reaction zone complex then propagates at this minimum velocity for a short period of the order of 10 μsec. The onset of instability is observed in the form of the appearance of local ignition centers. The rapid development of these local hot spots leads to a sudden transition to a highly asymmetrical multi-headed wave. From the experimental record of our previous paper [10], which was for stoichiometric O_2-C_2H_2 at 100 torr, the initiation energy $E_0 = 0.3$ joules and the value of $\Delta \simeq 2$ mm yielding a value of $\epsilon_c \simeq .18$. From Fig. 2 we note that this corresponds closely to the critical value of $\epsilon = 0.15$ for direct initiation to be possible.

For very small initiation energies (i.e., $\epsilon = \Delta/R_0$ is large), the wave decays below the specified limiting strength for auto-ignition (i.e., $M_C = 3$). The shock completely decouples from further chemical reactions and decays asymptotically to an acoustic wave $M_S = 1$. This regime is the so-called sub-critical energy regime defined in a previous paper [10].

From the present theory the critical energy for direct initiation E_c can be determined since the critical value of the initiation energy parameter $\epsilon_c = \Delta_c/R_{0c}$ is known. To evaluate E_c, we first compute $\Delta_c(p_0)$ using the formula of White (i.e., $\ln [C_2H_2]^{1/3}[O_2]^{1/3}\tau = -10.81 + 17300/4.58T$) based on the final steady state velocity $M_c = 3$. With $\Delta_c(p_0)$ known, the critical energy can be determined as follows:

$$\epsilon_c = \frac{\Delta_c(p_o)}{R_{oc}} = \frac{\Delta_c(p_o)}{\left(\frac{E_c}{4\pi\gamma p_o}\right)^{1/3}}$$

hence

$$E_c = \left(\frac{\epsilon_c}{\Delta_c(p_o)}\right)^3 \cdot 4\pi\gamma p_o$$

The dependence of E_c on p_o as well as $\Delta_c(p_o)$ from White's formula for the two cases of stoichiometric and equi-molar C_2H_2-O_2 mixtures are illustrated in Fig.3. The experimental points for the narrow pressure range .04 $\leq p_o \leq$ .15 atm. are taken from our previous paper [10] where a laser spark of 20 μsec. duration is used as the energy source. The agreement is quite reasonable in view of the uncertainty in the use of the kinetic data near the low temperature limit. It should be noted that although more data are available for the critical energy for direct initiation for these explosive mixtures, they cannot be used to compare with the present theoretical results. It was pointed out in a recent paper [10] that the critical energy can differ by a few orders of magnitude depending on the total discharge time. In order to compare with the present theoretical results based on a point blast model (i.e., $\frac{E_o}{\Delta t} \to \infty$), these existing data must be reduced to the limiting value corresponding to an infinite power density of the ignition source. Unfortunately, the details of the discharge characteristics for these experiments where the data are reported have not been stated to permit the appropriate data reduction. The laser spark is perhaps the most powerful point

energy source available which approximates closest to the theoretical requirement of point blast theory.

To confirm the existence of a final steady state velocity for spherical detonations that are below the classical value for the explosive, a comparison between the present results and the recent experimental data of Brossard [21] and Struck [22] is made. In Brossard's experiments, a 1 meter diameter spherical bomb is used and the detonation velocity is measured by the microwave doppler technique to an accuracy of 0.4%. Various mixtures (C_3H_8, H_2, C_2H_4, C_2H_2 with O_2) at an initial temperature of 293°K and $.1 \leq p_o \leq 2.8$ bar have been studied. In view of the large diameter chamber used to ensure steady state conditions as well as the accuracy of the wave velocity measurement by the doppler shift method, Brossard's results represent the most reliable existing data on spherical detonation velocities. In Struck's experiments, a much smaller chamber of 100.mm diameter was used. The detonation wave velocity was measured using high speed movie schlieren. The present theoretical results for $M_s^*(\epsilon, p_o)$ are shown in Fig. 4 for both stoichiometric and equi-molar C_2H_2-O_2 mixtures. In order to compare with Brossard and Struck's experimental data, the variations of M_s^* with initial pressure p_o for constant initiation energies E_o must be obtained. To derive these constant energy velocity curves, we proceed as follows: Suppose we desire $M_s^*(p_o)$ for a particular energy E_o. We note first of all that this curve must originate at the critical condition where $E_o = E_c$. From Fig. 3, the value of p_c and Δ_c can be obtained for any value of E_c. Hence at any pressure p_o, we may write

$$\epsilon(p_0) = \frac{\Delta_c(p_0)}{\left(\frac{E_0}{4\pi\gamma p_0}\right)^{1/3}} = \frac{\Delta_c(p_c)}{\left(\frac{E_0}{4\pi\gamma p_c}\right)^{1/3}} \cdot \frac{\Delta_c(p_0)}{\Delta_c(p_c)} \left(\frac{p_0}{p_c}\right)^{\frac{1}{3}}$$

hence

$$\epsilon(p_0) = \epsilon_c \frac{\Delta_c(p_0)}{\Delta_c(p_c)} \left(\frac{p_0}{p_c}\right)^{\frac{1}{3}}$$

For stoichiometric C_2H_2-O_2, $\epsilon_c = 0.15$ while for equi-molar mixtures, $\epsilon_c = 0.13$. Since M_s^* for various values of ϵ are determined from the solution, $M_s^*(p_0)$ of any particular value of E_0 can be derived. From Fig. 4 we note that the agreement between the present theory with the data of Brossard and Struck is quite good. It should be pointed out that from the present theory the detonation velocity depends only weakly on the initiation energy in the high pressure range $.55 \leq p_0 \leq 3$. Therefore although the initiation energy of both Brossard and Struck has not been properly reduced to the limiting value corresponding to infinite power density as required by the point blast model, the agreement is still very good.

Theoretical attempts [23, 24, 25] have been made to predict the cellular dimension of a multiheaded detonation front. Using the present theory, the longitudinal dimension of a "detonation cell" can be evaluated if it is assumed that the motion of a "detonation wavelet" in between collisions of transverse waves behaves like a decaying reacting blast as described by the present theory. Based on the experimental evidence that the minimum strength of a "detonation wavelet" just prior to the re-energization by the collision of a pair of transverse waves

is about $M_s \simeq 3$ which corresponds to the critical limiting strength for auto-ignition, we shall take the shock radius z_c for the case where $\epsilon = \epsilon_c$ as the longitudinal dimension of the detonation cell. From Fig. 2, we note that $z_c \simeq .6$ and the value of $\epsilon_c \simeq .15$. These values (i.e., ϵ_c, z_c) are almost the same for a wide pressure range for stoichiometric C_2H_2-O_2 mixtures while for equi-molar mixtures $\epsilon_c \simeq .13$ and $z_c \simeq .6$. Using these values, the longitudinal cell dimension R_d can be obtained through the relationship

$$R_d = z_c \frac{\Delta_c(p_o)}{\epsilon_c}$$

Using White's formula to determine $\Delta_c(p_o)$, the variation of R_d with initial pressures p_o can be obtained. To compare with the experimental data of Strehlow [26], the longitudinal dimension must be multiplied by a factor of about 0.62 based on the definition he used for the transverse wave spacing. This comparison is shown in Fig. 5 and, as can be observed, the agreement is reasonable. It should be pointed out that there is no concrete experimental evidence to support the assumption that the motion of a detonation wavelet can be modelled by a point blast wave. In fact, as Strehlow pointed out, the center of curvature of the detonation wavelet does not corespond to the point of collision of the transverse wave where the "decaying wavelet" first originates. Also, the impulsive release of energy by the collision of transverse waves is by no means instantaneous. Hence the subsequent decay of the "wavelet" does not correspond to that from the present model. However, in view of the similarity in the gross features of the decay

processes between experiments and the present theory, it seems reasonable to adopt the blast wave model as a first approximation.

5. Conclusions

It should be emphasized that the most important results of the present theory are that it predicts the existence of steady state sub-Chapman-Jouguet velocities which depend on the details of the initiation processes. In other words, the final steady motion of the detonation front bears the memory of the initiation condition through the hydrodynamic flow structure generated by the ignition source. This is supported by the recent accurate experimental measurements made by Brossard. If the present theory, together with Brossard's as well as Struck's experimental results, are to be taken as correct, then the classical Chapman-Jouguet theory of detonation waves must be modified. The abundance of the experimental results gathered in the past decade strongly indicates the inadequacy of the Chapman-Jouguet theory. The recent verbal critique of the Chapman-Jouguet theory by Professor Manson at the 13th Combustion Symposium emphasizes the importance of the influence of the hydrodynamic flow structure in the wake of the expanding detonation on its motion. The present theory can be considered as a particular case where the hydrodynamic flow structure is peculiar to that of a point energy source. It would be important to extend the present model to other types of hydrodynamic flow structure in order to establish whether the predictions from the present model are indeed universal. Equally important will be more careful experiments on spherical detonations in the low pressure, low initiation regime where the effects of the experiments can be manifested in a more pronounced fashion.

6. Acknowledgements

This study is supported by the National Research Council of Canada under Grant No. A-3347, A-118, and AFOSR Contract 69-1752B.

7. References

1. JOUGUET, M., Comptes Rendus 142, 1034 (1906).

2. TAYLOR, G.I., Proc. Roy. Soc. (London) A200, 235 (1950).

3. ZELDOVICH, Ia. B. and KOMPANEETS, A.S., "Theory of Detonation", Academic Press (1960).

4. LEE, J.H., McGill University Rept. 65-1 (1965).

5. KOROBEINIKOV, V.P., Astronautica Acta, Vol. 14, pp. 411-419 (1969).

6. LEVIN, V.A. and CHERNYI, G.G., P.M.M., Vol. 31, No. 3, pp. 393-405 (1967).

7. LEE, J.H., KNYSTAUTAS, R. and BACH, G.G., "Theory of Explosions", McGill University Rept. 69-10 (1969); also AFOSR 69-3090 TR.

8. FICKETT, W. and WOOD, W.W., Physics of Fluids 9, 903 (1966).

9. STREHLOW, R.A. and HARTUNG, W., Combustion and Flame 9, 423 (1965).

10. BACH, G.G., KNYSTAUTAS, R. and LEE, J.H., Twelfth Symposium (International) on Combustion, p. 853, The Combustion Institute (1969).

11. LUNDSTROM, G.A. and OPPENHEIM, A.K., Proc. Roy. Soc. A310, 463 (1969).

12. RAJAN, S., University of Illinois Tech. Rept. AAE 70-1 (1970).

13. TAKI, S. and FUJIWARA, T., Thirteenth Symposium (International) on Combustion, p. 1119. The Combustion Institute (1971).

14. BACH, G.G., GUIARO, C., KNYSTAUTAS, R. and LEE, J.H., Bull. of the Am. Phys. Soc., Nov. 1970, p. 1536.

15. BACH, G.G., KNYSTAUTAS, R. and LEE, J.H., Thirteenth Symposium (International) on Combustion, p. 1097. The Combustion Institute (1971).

16. SAKURAI, A., J. of Phys. Soc. of Japan, Vol. 8, pp. 662-669 (1953); ibid. Vol. 9, No. 2, pp. 256-266 (1954).

17. OSHIMA, K., University of Tokyo, Aero. Res. Inst., Rept. No. 358 (1960); see also "Exploding Wires" (ed. by W.G. Chase and H.K. Moore), Plenum Press, N.Y., Vol. 2, pp. 159-180 (1962).

18. BACH, G.G. and LEE, J.H., AIAA Journal, Vol. 8, No. 2, pp. 271-275 (Feb. 1970).

19. SHCHELKIN, K.J., Dokalady Akad. Nauk. SSSR., Vol. 160, No. 5, pp. 1144-1146 (1965).

20. WHITE, D.R., Eleventh Symposium (International) on Combustion, p. 147, The Combustion Institute, Pittsburgh (1967).

21. BROSSARD, J., "Contribution à l'etude des ondes de choc et de combustion spheriques divergentes dans les gaz", theses de doctorat, Faculte des Sciences, Universite de Poitiers (1970).

22. STRUCK, W., "Kugelformige Detonationswellen in Gasgernischen", Doctoral dissertation, Fac. of Math., Natl. Sciences Tech. University, Hachen (1968); (see also comments by Struck in the Eleventh Symposium (International) on Combustion, p. 862 (1969).

23. MANSON, N., Compt. Rend. 222, 46 (1946).

24. FAY, J.A., J. Chem. Phys. 20, 942 (1952).

25. STREHLOW, R.A., "Fundamentals of Combustion", pp. 313 328, Int. Textbook Co. (1968).

26. STREHLOW, R.A. and ENGEL, G.D., AIAA Journal 7, 492 (1969).

8. Figure Captions

Fig. 1 The solutions of $\eta(\bar{z})$, $\theta(\bar{z})$, $S^2(\bar{z})$ and $\eta'(\bar{z})$ for various values of ξ for stoichiometric C_2H_2-O_2 mixtures at p_o = 100 torr, T_o = 300°K.

Fig. 2 The variation of shock strength M_s with shock radius for various values of ξ (stoichiometric C_2H_2-O_2, p_o = 100 torr, T_o = 300°K).

Fig. 3 The variation of the critical energy E_c for direct initiation and the critical induction zone thickness Δ_c with initial pressures for stoichiometric and equi-molar C_2H_2-O_2 mixtures.

Fig. 4 Comparison of the detonation velocities in stoichiometric and equi-molar C_2H_2-O_2 mixtures with the experimental data of Brossard (Ref. 21) and Struck (Ref. 22).

Fig. 5 Comparison of the predicted transverse wave spacings with the experimental data of Strehlow (Ref. 26).

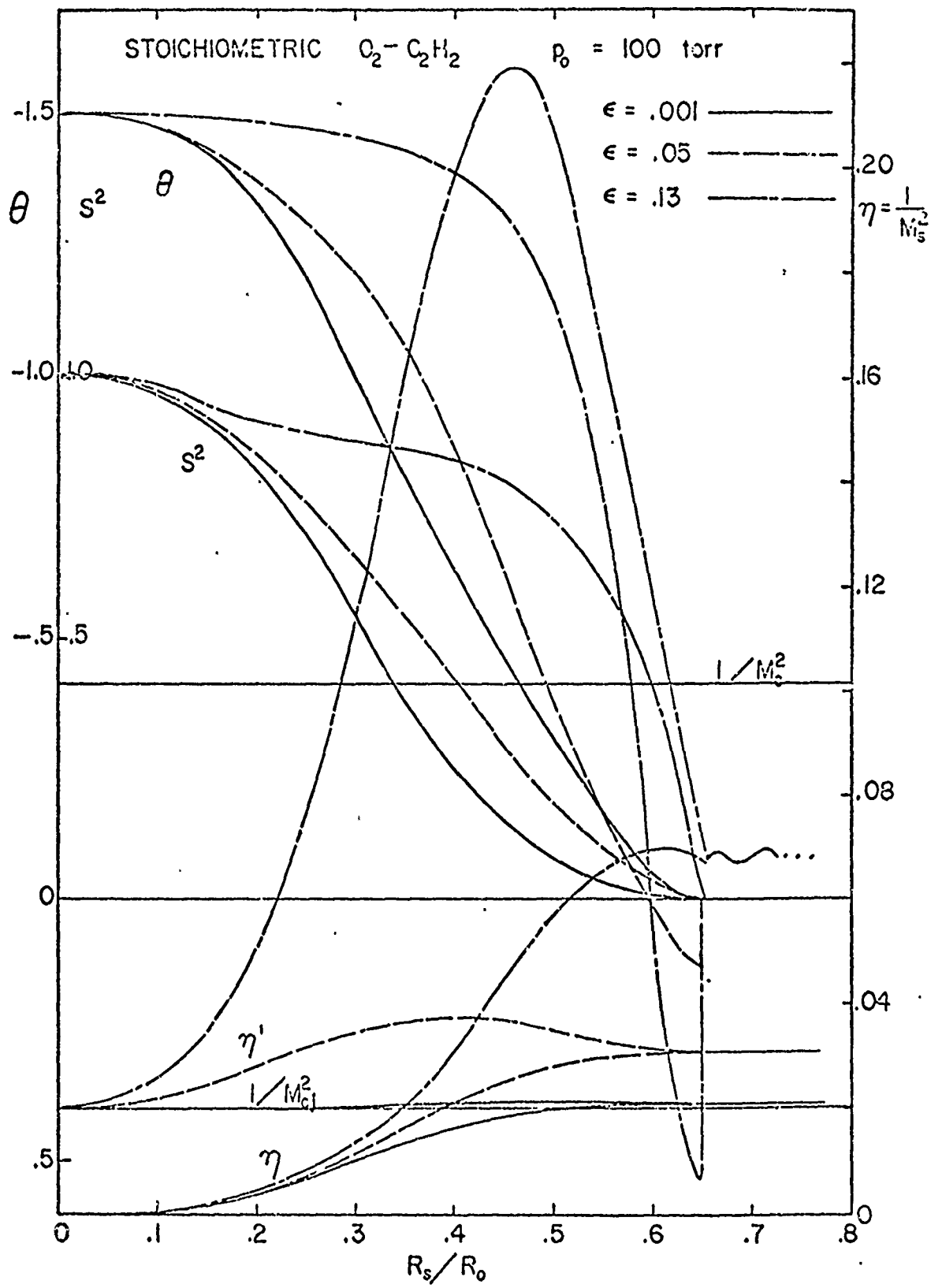
STOICHIOMETRIC $C_2 - C_2H_2$
p_o = 100 torr
ϵ = .001
ϵ = .05
ϵ = .13
θ
S^2
θ
S^2
$\eta = \frac{1}{M_s^2}$
$1/M_c^2$
η'
$1/M_{c_1}^2$
η
-1.5
-1.0
-.5
0
.5
1.0
.5
.20
.16
.12
.08
.04
0
0
.1
.2
.3
.4
.5
.6
.7
.8
R_s/R_o

FIG. 1

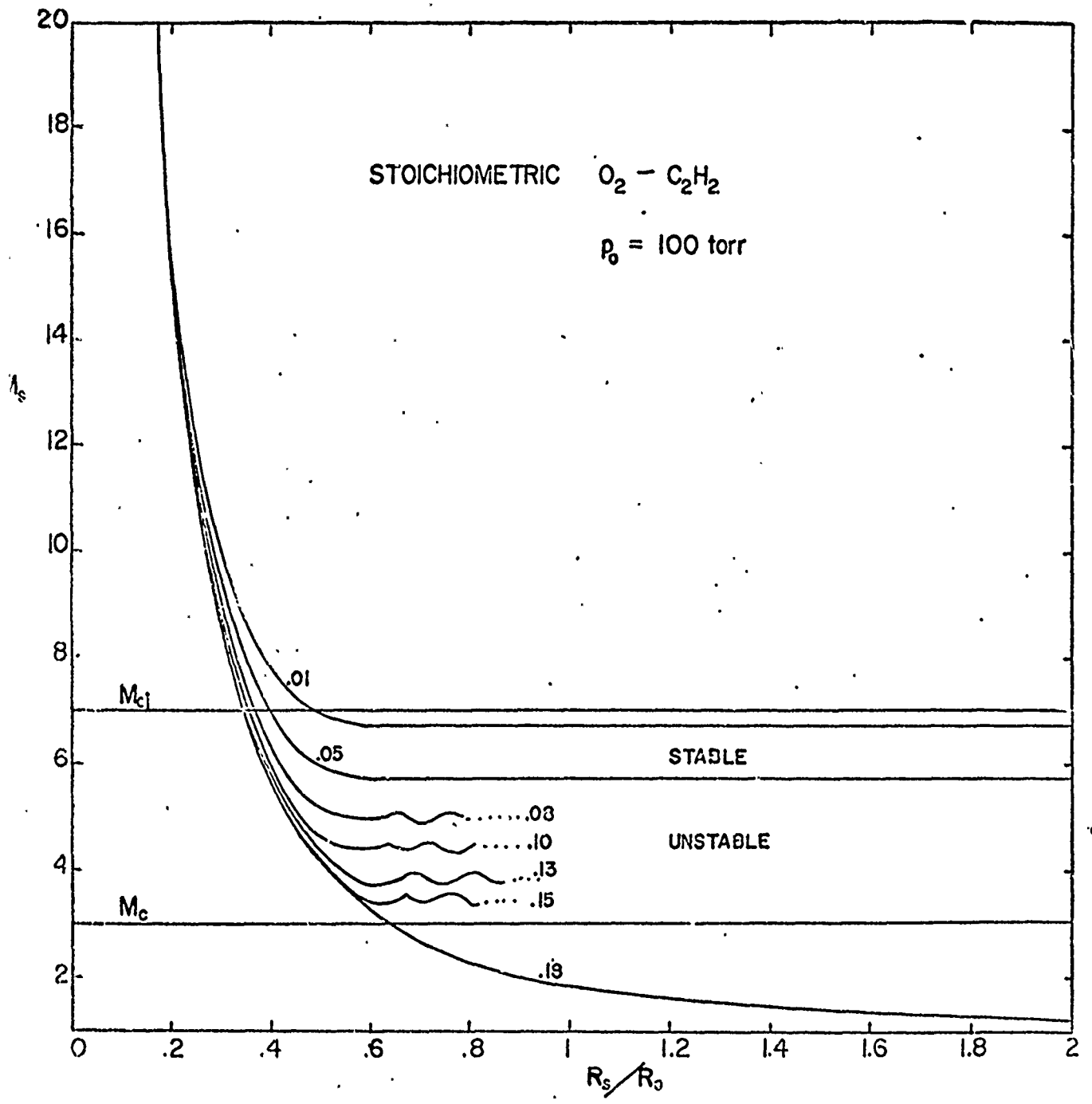
STOICHIOMETRIC $O_2 - C_2H_2$
p_o = 100 torr
M_s
M_{cj}
M_c
.01
.05
.08
.10
.13
.15
.18
STABLE
UNSTABLE
20
18
16
14
12
10
8
6
4
2
0
.2
.4
.6
.8
1
1.2
1.4
1.6
1.8
2
R_s/R_o

FIG. 2

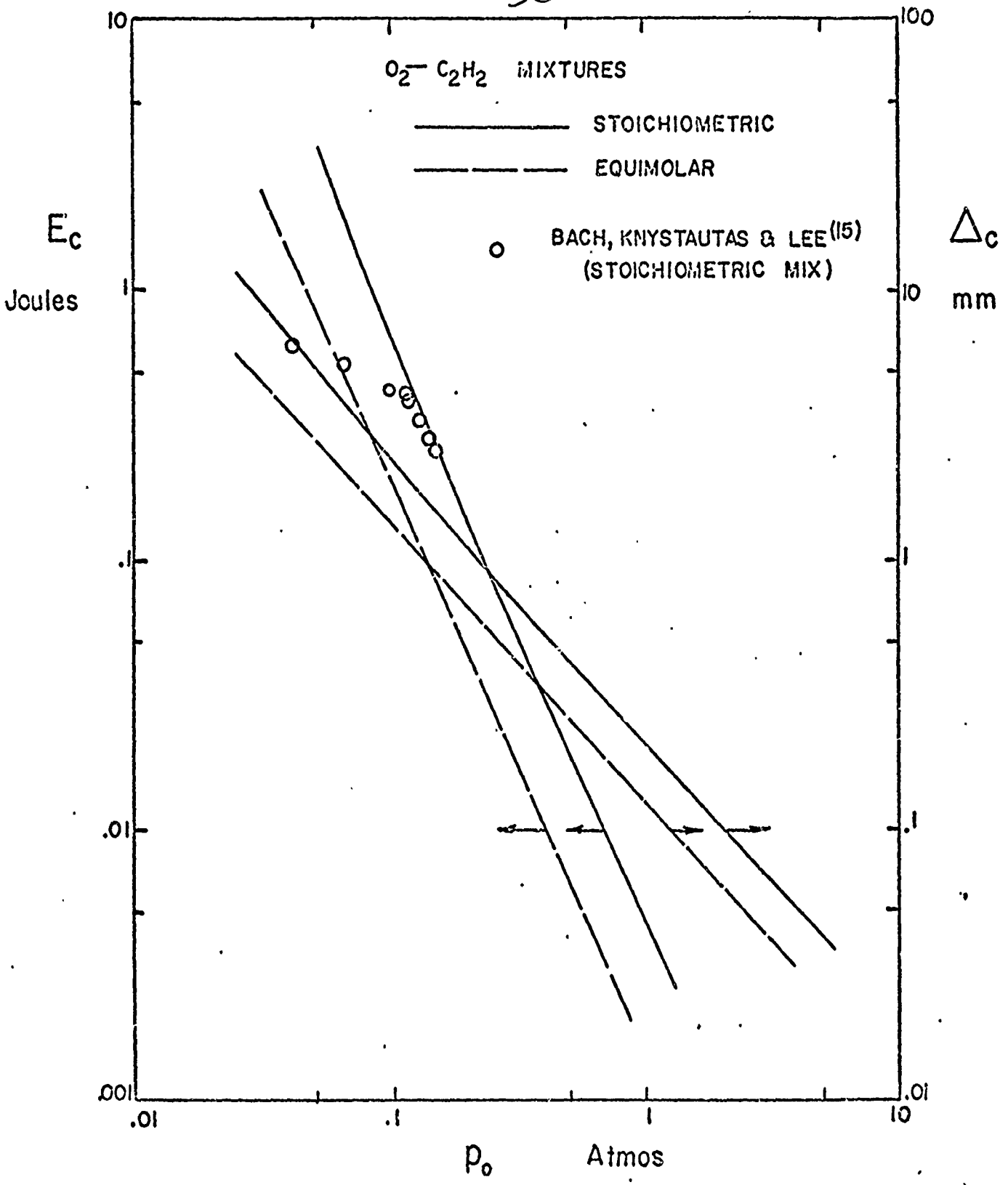
O_2 — C_2H_2 MIXTURES
STOICHIOMETRIC
EQUIMOLAR
BACH, KNYSTAUTAS & LEE[15]
(STOICHIOMETRIC MIX)
E_c
Joules
Δ_c
mm
10
1
.1
.01
.001
100
10
1
.1
.01
.01
.1
1
10
p_o Atmos

FIG·3

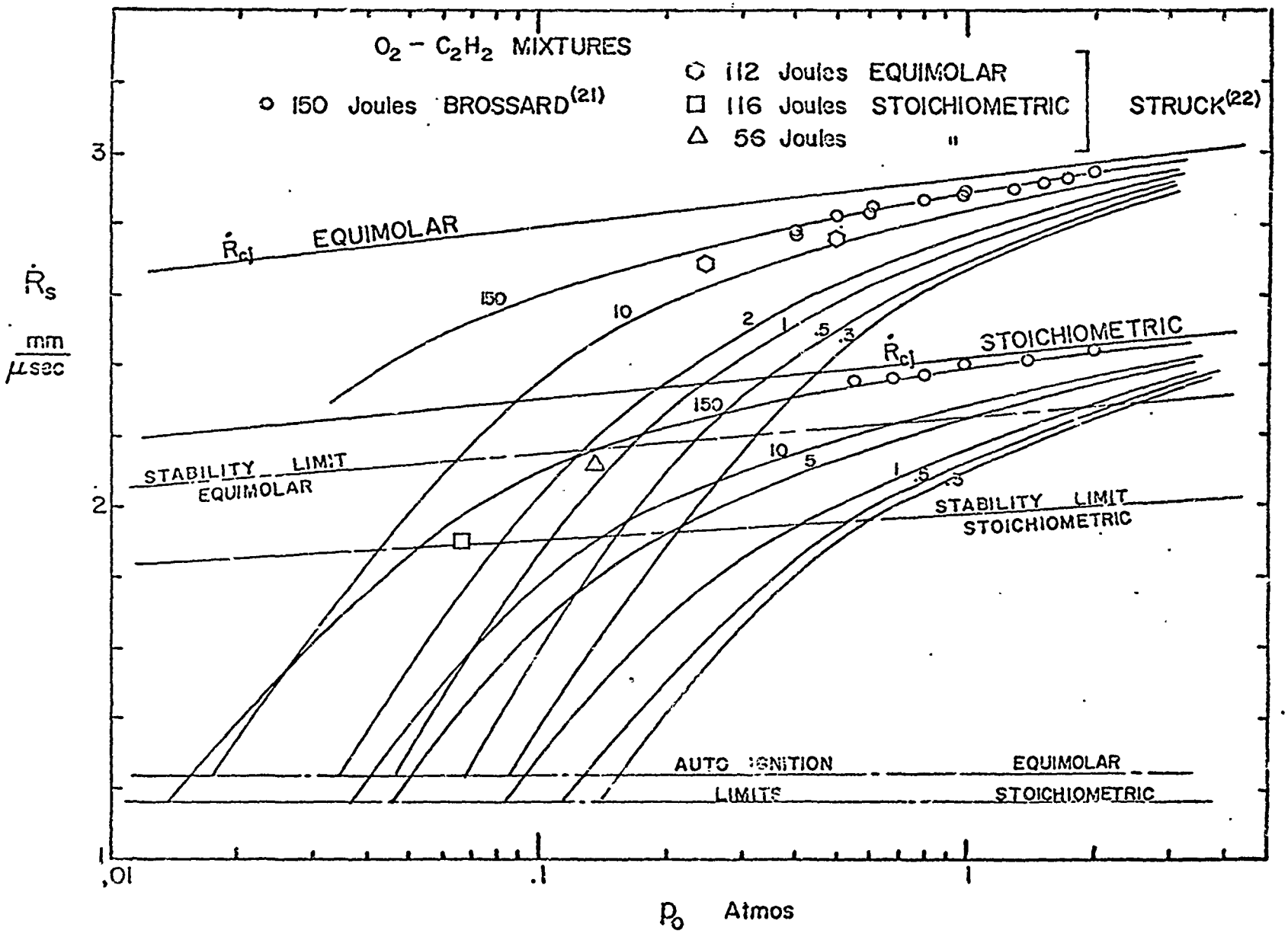
$O_2 - C_2H_2$ MIXTURES
150 Joules BROSSARD(21)
112 Joules EQUIMOLAR
116 Joules STOICHIOMETRIC
56 Joules "
STRUCK(22)
$\dot{R}_s$ mm/μsec
$\dot{R}_{cj}$ EQUIMOLAR
150
10
2
1
.5
.3
$\dot{R}_{cj}$ STOICHIOMETRIC
150
10
5
1
.5
.3
STABILITY LIMIT EQUIMOLAR
STABILITY LIMIT STOICHIOMETRIC
AUTO IGNITION LIMITS
EQUIMOLAR
STOICHIOMETRIC
3
2
1
.01
.1
1
p_o Atmos

FIG-4

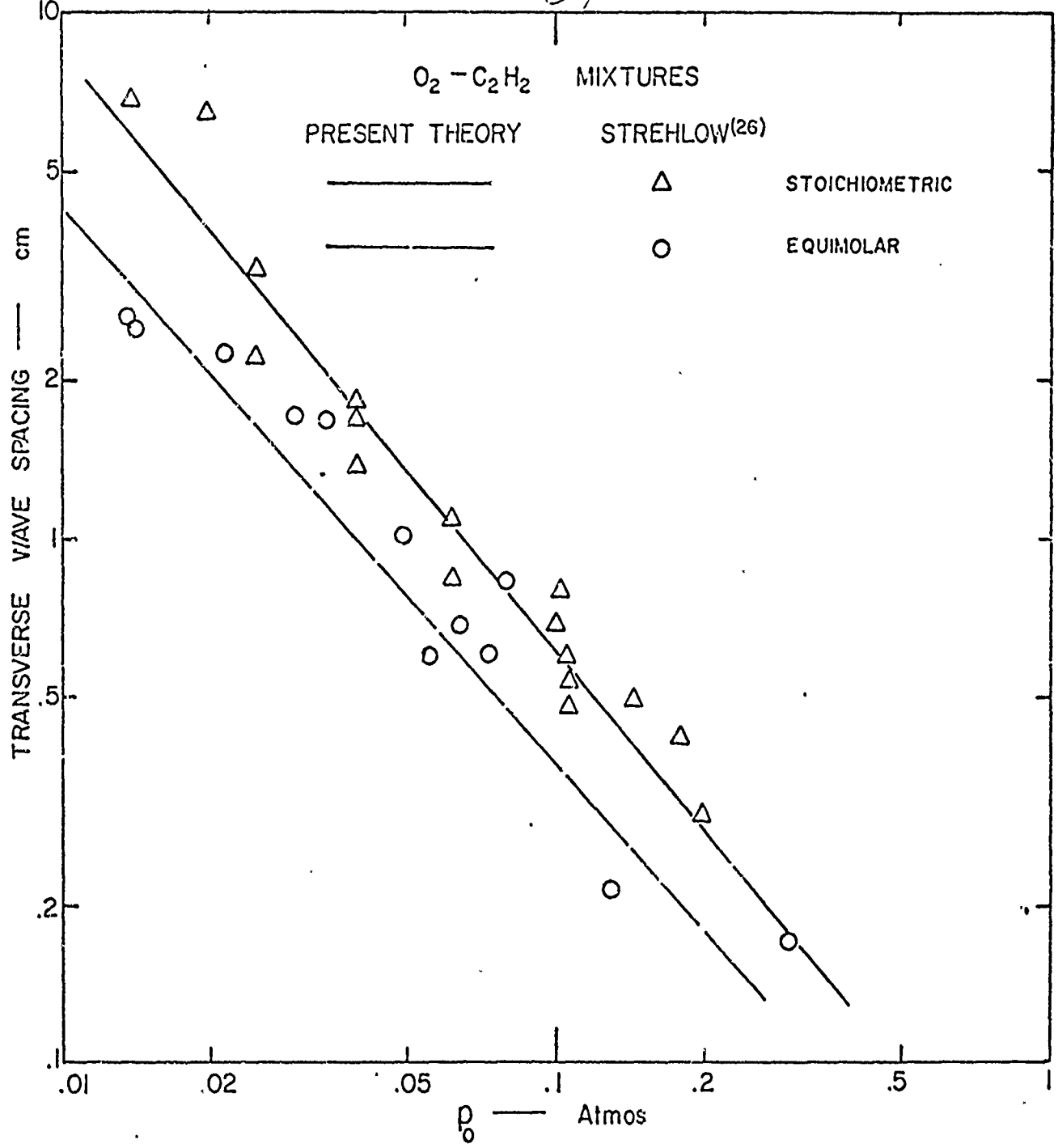
$O_2 - C_2H_2$ MIXTURES
PRESENT THEORY
STREHLOW(26)
STOICHIOMETRIC
EQUIMOLAR
TRANSVERSE WAVE SPACING — cm
10
5
2
1
.5
.2
.1
.01
.02
.05
.1
.2
.5
1
p_0 — Atmos

FIG. 5